Towards Automatic Collateral Circulation Score Evaluation in Ischemic Stroke Using Image Decompositions and Support Vector Machines

Yiming Xiao[1,2(✉)], Ali Alamer[3], Vladimir Fonov[4], Benjamin W.Y. Lo[5], Donatella Tampieri[3,5], D. Louis Collins[4], Hassan Rivaz[1,2], and Marta Kersten-Oertel[1,6]

[1] PERFORM Centre, Concordia University, Montreal, Canada
yiming.xiao@concordia.ca
[2] Department of Electrical and Computer Engineering, Concordia University, Montreal, Canada
[3] Diagnostic and Interventional Neuroradiology, Montreal Neurological Hospital, Montreal, Canada
[4] McConnell Brain Imaging Centre, Montreal Neurological Institute, Montreal, Canada
[5] Department of Neurology and Neurosurgery, Montreal Neurological Hospital, Montreal, Canada
[6] Department of Computer Science and Software Engineering, Concordia University, Montreal, Canada

Abstract. Stroke is the second leading cause of disability worldwide. Thrombectomy has been shown to offer fast and efficient reperfusion with high recanalization rates and thus improved patient outcomes. One of the most important indicators to identify patients amenable to thrombectomy is evidence of good collateral circulation. Currently, methods for evaluating collateral circulation are generally limited to visual inspection with potentially high inter- and intra-rater variability. In this work, we present an automatic technique to evaluate collateral circulation. This is achieved via low-rank decomposition of the target subject's 4D CT angiography, and using principal component analysis (PCA) and support vector machines (SVMs) to automatically generate a collateral circulation score. With the proposed automatic score evaluation technique, we have achieved an overall scoring accuracy of 82.2% to identify patients with poor, intermediate, and good/normal collateral circulation.

Keywords: CTA · Collateral score · Stroke · Machine learning

1 Introduction

According to the World Heart Federation, each year over 15 million people suffer from brain stroke, with 6 million dying as a result, and 5 million becoming permanently disabled[1]. The two main types of stroke are: (1) hemorrhagic, due to bleeding, and (2) ischemic, due to a lack of blood flow. In this paper, we focus on ischemic stroke, which

[1] http://www.world-heart-federation.org/cardiovascular-health/stroke/.

M.J. Cardoso et al. (Eds.): CMMI/RAMBO/SWITCH 2017, LNCS 10555, pp. 158–167, 2017.
DOI: 10.1007/978-3-319-67564-0_16

accounts for approximately 87% of all stroke cases. In ischemic stroke, where poor blood flow to the brain causes neuronal cell death, the goal of treatment is to restore blood flow to preserve tissue in the ischemic penumbra, where blood flow is decreased but sufficient enough to stave off infarction (i.e. cell death).

It has been shown that recanalization, i.e. restoring blood flow, is the most important modifiable prognostic predictor for a favorable outcome in ischemic stroke [1]. Timely restoration of regional blood flow can help salvage threatened tissue, reducing cell death, and ultimately minimizing patient disabilities. Thrombectomy, where a long catheter with a mechanical device attached to the tip, is used to remove a clot, has been effective for treatment for ischemic stroke. However, the inherent risks associated with thrombectomy must be considered, and only patients with certain indications, including a large penumbra, small infarct, and sufficient collateral circulation should undergo such interventions. Collateral circulation (i.e., collaterals) is defined as a supplementary vascular network that is dynamically recruited when there is an arterial occlusion (e.g. a clot) and has been shown to be one of the most important factors in determining treatment strategies [2, 3].

Currently, collaterals are typically evaluated on Computed Tomography Angiography (CTA) or Magnetic Resonance Angiography (MRA), however, there is no consensus on which imaging modality should be used [4]. For assessment on CTA, a collateral score is based on visual inspection of the images by a radiologist and can be graded using scoring systems, such as the Alberta Stroke Program Early CT Score (ASPECTS) [5]. However, visual inspection is often subject to inter- and intra-rater inconsistency and can be time-consuming. To the best our knowledge, no automatic collateral score evaluation methods have been reported previously in the literature.

In this paper, we present an automatic technique for estimating the collateral score in dynamic 4D CTA images. First, blood vessel patterns are extracted using low-rank image decompositions, and then collateral scores are assigned using support vector machines (SVMs) based on eigen blood vessel patterns from principal component analysis (PCA). To demonstrate the performance of SVMs for the task, we compared the results against classification using k-nearest neighbors (kNN) and random forests.

2 Materials and Methods

2.1 Subjects and Scanning Protocols

For this study, we included 29 patients who had suffered a stroke and 8 healthy subjects. For all subjects (age $= 65 \pm 15$ yo), isotropic computed tomography (CT) imaging was acquired on Toshiba's Aquilion ONE 320-row detector 640-slice cone beam CT (Toshiba medical systems, Tokyo, Japan). The time between symptoms onset and scanning varies, but for most it is within 24 h. The routine stroke protocol uses a series of intermittent volume scans over a period of 60 s with a scanning speed of 0.75 s/rotation. This protocol provides whole brain perfusion and whole brain dynamic vascular analysis in one examination. A total of 18 volumes are acquired, where a series of low-dose scans are performed: first for every two seconds during the arterial phase, and then spaced out to every 5 s to capture the slower venous phase of the contrast bolus. Isovue-370

(Iopamidol) is used as non-ionic and low osmolar contrast medium (Iodine content, 370 mg/ml).

2.2 Collateral Circulation Scoring for Patients

The collateral circulations of the 29 patients were scored by two radiologists as being *good*, *intermediate* or *poor* using the Alberta Stroke Program Early CT score (ASPECTS) [5]. The scoring criteria are as follows: a score of *good* is given for 100% collateral supply of the occluded middle cerebral artery (MCA) territory; *intermediate* score is given when collateral supply fills more than 50% but less then 100% of the occluded MCA territory; a *poor* score indicates collateral supply that fills less then 50% but more than 0% of the occluded MCA territory (Fig. 1). Among the patients, we had 9 *good*, 14 *intermediate*, and 6 *poor* subjects.

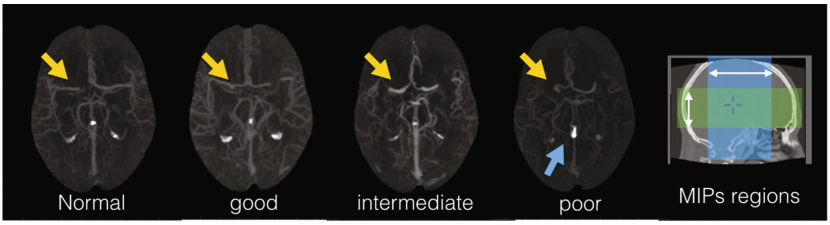

Fig. 1. Examples of axial maximum intensity projections (MIPs) for different collateral circulation scores. The middle cerebral artery (MCA) is annotated with yellow arrows, and the blue arrow points to calcification at the pituitary gland. The MCA territory is to the lateral region of the MCAs. The blue and green regions are the projection regions in the coronal and axial directions that will be used for automatic collateral score computation. (Color figure online)

2.3 Image Processing

Each subject's 18 CTAs were first rigidly co-registered together, and then spatially normalized to a population-averaged CTA template created using the first CTA of the series (with the least blood vessel contrast) with nonlinear registration. The registrations help ensure all brains were in the same space for analysis, and were completed with the freely available Advanced Normalization Tools (ANTs) (stnava.github.io/ANTs). The template was created from 11 healthy subjects that had undergone the same dynamic 4D-CTA imaging protocol. Individual averaged CTAs were deformed and averaged together through an unbiased group-wise registration scheme as described in [6]. The resulting template, with a resolution of $1 \times 1 \times 1$ mm^3, is shown in Fig. 2. A brain mask was extracted from the template using the active contour segmentation tool in ITK-SNAP (www.itksnap.org) and used for the analysis of individual brain volumes.

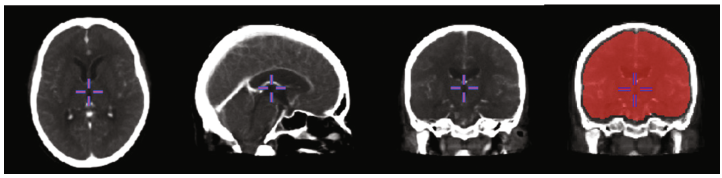

Fig. 2. Population-averaged non-linear template (From left to right: axial, sagittal and coronal views). The brain mask is shown overlaid on the coronal view in the rightmost image.

2.4 Blood Vessel Extraction

The evaluation of collateral circulation is largely determined by the flow of contrast agent in the blood vessels over time. However, within the CTA images, other brain anatomy, such as the ventricles and grey matter are still visible. To remove non-vessel structures that exhibit inter-subject variability and can affect the PCA results intended only for blood vessels, we employed low-rank decomposition. Previously, low-rank decomposition has been used to separate foreground and background in a scene from video footages [7]. In this case, each image in the series can be modeled as the summation of the low-rank components that contain consistent anatomical structures across time, and a sparsity term that describes the intensity changes in the blood vessels. For a subject k, the 4D CTAs are stored in a matrix $D = \left[I_k^1, .., I_k^i, \ldots, I_k^{18}\right]$, where I_k^i is the i^{th} CTA image that is converted to a column vector from the time series. The low-rank representation of D is defined as:

$$\left\{\widehat{L}, \widehat{S}\right\} = argmin_{L,S}\left(rank(L) + \gamma \|S\|_0\right) \; subject\; to\; D = L + S \tag{1}$$

where $\|S\|_0$ is the counting norm of the sparsity component S, rank(L) is the matrix rank of the low-rank component L, and γ is a positive scalar. To make the optimization tractable, the problem is then transformed as:

$$\left\{\widehat{L}, \widehat{S}\right\} = argmin_{L,S}\left(\|L\|_* + \rho \|S\|_1\right) \; subject\; to\; D = L + S \tag{2}$$

where $\|L\|_*$ is the nuclear norm of L, $\|S\|_1$ is the L1-norm of S, and ρ is a positive scalar that controls the approximated rank of matrix L. There have been many methods to solve this optimization problem. For our application, we employed the augmented Lagrange multiplier method [8] to recover the low-rank and sparsity components. As a result, each image I_k^i is represented as $I_k^i = l_k^i + s_k^i$, where l_k^i and s_k^i are the low-rank and sparse representation of I_k^i. For our application, to reduce image noise and inter-subject anatomical variability (i.e., blood vessels), the CTA images were first blurred by a Gaussian kernel of $\sigma = 3$ mm (the thickness of main arteries), and then processed with low-rank decomposition. All sparse representations for each subject's CTA series were averaged. Lastly, the median value projection in the axial direction and mean value projection in the coronal direction were obtained using the projection regions in Fig. 1. They were then

used to extract eigen vessel patterns. Examples of the projections are shown in Fig. 3. Note that on the left hemisphere, as the blood circulation worsens, the intensity of the blood vessels becomes lower.

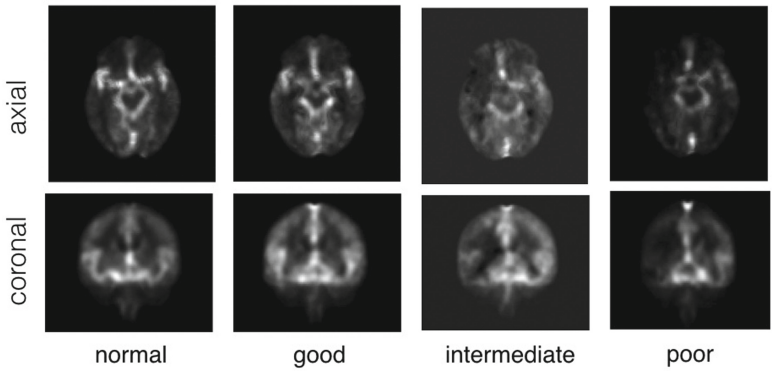

Fig. 3. Examples of 2D projection images (axial view: median value in axial direction, coronal view: mean value in coronal direction) for the typical normal, good, intermediate and poor collateral circulation.

2.5 Eigen Vessel Patterns and Score Assignment

Principal component analysis (PCA) has been commonly used for object recognition [9] through the generation of eigen image basis. From the training set composed of selected vectorized image features $X = [X_1, X_2, \ldots, X_m] \subset \Re^{n \times m}$, the covariance matrix C can be decomposed into $C = U \Lambda U^T$, with Λ being the diagonal matrix containing the eigenvalues $\{\lambda_a\}_{a=1\ldots N}$ and U being the orthonormal matrix that has the corresponding principal components (or eigen vessel patterns) $\{\emptyset_a\}_{a=1\ldots N}$. When a new image ψ is presented, it can be represented as $\psi = \overline{X} + \sum_{a=1}^{N} w_a \phi_a$, where the reconstruction coefficient can be found via $w_a = \phi_a^T \left(\psi - \overline{X}\right)$ and $\overline{X} = \frac{1}{m} \sum_{j=1}^{m} X_j$. As we have images from coronal and axial direction projections for subject k, two sets of reconstruction coefficients $\boldsymbol{w}^k_{coronal}$ and $\boldsymbol{w}^k_{axial}$ were concatenated as $\boldsymbol{w}^k = \left[\boldsymbol{w}^k_{coronal}, \boldsymbol{w}^k_{axial}\right]$ to feed into multi-class SVMs with the radial basis function (RBF) kernel and one-vs-all scheme [10] to assign each subject with a collateral score. For a binary SVM classifier, the decision function is defined as $f(\boldsymbol{w}) = \sum y_i \alpha_i K\left(\boldsymbol{w}, \boldsymbol{w}_i\right) + b$, where the kernel $K\left(x_i, x_j\right) = \exp\left(\beta \left\| x_i - x_j \right\|^2\right)$ is the radial basis function, $\boldsymbol{w}_i$ is the support vector, y_i is the binary class label, and α_i and b are the coefficients and bias term to be trained. In the one-vs-all type scheme, a binary SVM is trained for each class to separate the examples in the target class (positive labeled) from the remaining ones (negative labeled). For a

new subject to be classified, the axial and coronal projection images are first projected to the eigen vessel patterns obtained from the training data, and the associated feature vector $\boldsymbol{w}$ is produced by concatenating the reconstruction coefficients. Lastly, the feature vector $\boldsymbol{w}$ is classified with the associated classifier that has the highest score computed from all classifiers.

2.6 Training and Validation

As there is almost no visual difference between the 4D CTAs of normal controls and patients with collateral scores of good, we combined them as one group for training and classification. Therefore, we categorized all the subjects into three classes: good/normal, intermediate, and poor. As there are much fewer subjects with poor collateral circulation and it is desirable to have a balanced dataset for training, we generated 8 more new subjects by nonlinearly registering these cases to normal controls with the least anatomical similarity to them. We used CTA images that contain general brain anatomy and clear vasculature for registration. This way, we ensure that the synthesized anatomy is distinct from both the original image and the image to be registered to. To further enrich the training set, we also included the left-and-right mirrored versions of the subjects since most often a stroke occurs unilaterally, and the equal chance of having a stroke on the left or right hemisphere should be represented. Finally, we employed a leave-one-out scheme to validate our computer-assisted scoring system. However, as the dataset contains both the original and mirrored images, we only validated the classification results for 45 original images in order to avoid repeated classification. More specifically, for each target subject to receive a score, the subject's images (both original and mirrored versions) will be excluded from the training set. This leaves 88 subjects to generate the eigen vessel patterns and train the classifier at each round of validation. To assess the performance of the SVMs for collateral scoring, with the same image features, we compared the classification results using SVMs against those using k-nearest neighbors (kNN) and random forests. More specifically, through cross-validation, in terms of overall scoring accuracy, we found that for kNN, the optimal number of neighbors is 7, and for random forests, 150 trees offer the best results.

3 Results

3.1 Low-Rank Image Decomposition

A demonstration of low-rank decomposition is shown in Fig. 4 for two different subjects. Compared with the original image, the pattern of blood vessels is captured in the sparsity component while the other brain anatomy and calcification in the falx (Subject 1) have been removed. As for Subject 2 with poor collateral circulation, the absence of bright blood vessels on the right hemisphere can be observed in the sparsity component.

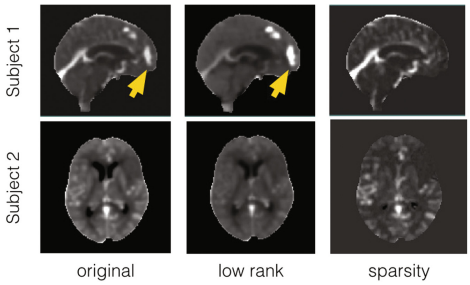

Fig. 4. Demonstration of low-rank decomposition using two subjects (different from those in Fig. 3). The yellow arrows point to the calcifications, and the vasculatures are shown as bright signals in the sparsity images. (Color figure online)

3.2 Eigen Vessel Patterns

The first 5 most significant principal components (or eigen vessel patterns) ranked by the eigenvalues for the two projections are shown in Fig. 5. Note that the asymmetric eigen vessel patterns in Fig. 5 are the results of unilateral collateral clots.

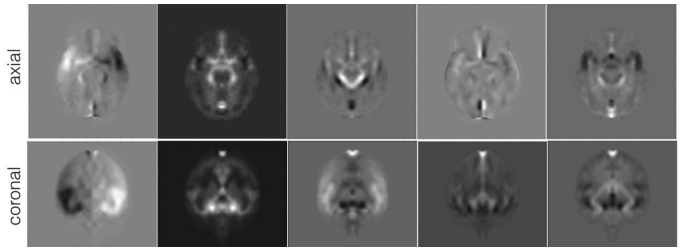

Fig. 5. Eigen blood vessel patterns of axial and coronal projection images.

3.3 Automatic Collateral Circulation Scoring Results

The score assignment accuracy for each class and in total are show in Table 1 for the SVMs, random forests, and k-nearest neighbors. In general, the SVMs achieved higher scoring accuracy than the other two methods. To better understand the classification results with SVMs, the related confusion matrix is shown in Table 2.

4 Discussion and Future Work

We used low-rank decomposition to extract vasculatures from the 4D CTA for three reasons. First, compared with simple subtraction of pre- and post-contrast CTAs, low-rank decomposition does not increase the image noise level. Second, the method can remove or mitigate unwanted image features, such as hyperintense signals from the calcifications in the pituitary gland, ventricles or the falx. Lastly, the method preserves

the relative image intensity changes due to blood circulation while removing other anatomical features. We employed 2D projection images for the classification task. Compared with directly using 3D volumes, which achieved overall scoring accuracy of 73.3%, 46.7% and 46.7% for SVMs, random forests, and kNN techniques, respectively, the 2D approach requires less computational burden, and performs better likely due to further reduction of blood vessel anatomical variability from projection. Here, the projection methods are chosen with the consideration of the blood flow direction (from bottom to top of the brain). When a clot occurs, the superior side of the MCA territory will appear dark, and the more severe the case is, the less blood reaches the region. As a result, the coronal mean projection captures the blood supply perpendicular to the flow direction while the axial median projection measures the property along flow direction. Compared with the selected projection methods, the conventional MIPs did not perform as well (71.1%, 55.6%, and 57.8% overall classification accuracy for SVMs, kNN, and random forests).

Table 1. Evaluation of collateral circulation score classification accuracy

	Normal/Good	Intermediate	Poor	All
SVMs	82.4%	64.3%	100%	82.2%
Random forest	64.7%	42.9%	85.7%	64.4%
kNN	41.2%	42.9%	85.7%	55.6%

Table 2. Confusion matrix for collateral score classification results using SVMs.

Prediction	True class		
	Normal/Good	Intermediate	Poor
Normal/Good	14	2	0
Intermediate	2	9	0
Poor	1	3	14

For this work, we only had a small cohort of subjects available, yet the cerebral vasculature has much higher variability than other anatomical structures in the brain. Therefore, we blurred the CTA images using a Gaussian kernel with a kernel size of 3 mm, which is the diameter of the main cerebral arteries, to reduce the variability of the smaller vessels. For training, we synthesized new subjects with poor collateral circulation due to a highly imbalanced dataset. Since nonlinear registration will significantly alter anatomical features, rendering the synthesized datasets sufficiently different from both the original and the image to be registered, they were included in cross-validation. With more subjects, the classification results may be further improved, and we could explore the popular convolutional neural networks to inspect the feature space and potentially improve the classification. Another limitation of the current techniques comes from the inter- and intra-variability of the scores in practice. With simple visual inspection of 3D data, it is challenging to establish consistent and accurate scores particularly for images that appear in between the categories (e.g., intermediate vs. good). This may partially contribute to the lower classification accuracy for the intermediate

class, as many from the group were assigned to good/normal or poor groups. In addition, in contrast to the good/normal and poor collateral scores, the wider range of variability among the population of intermediate collateral circulation also contributes to the lower classification accuracy. However, in clinical practice, it is most important to differentiate between good and intermediate collaterals versus poor collateral circulation since in individuals with poor collaterals the results of thrombectomy are poor. In the future, we will conduct evaluation on the inter- and intra-rater variability in labelling collaterals, and further validate our technique in relation to such information. Although averaging the extracted blood vessels for each subject can help gain information regarding blood flow over time, we would like to explore other techniques that explore temporal information, as well as more advanced rank-reduction techniques that better preserve relevant features for more accurate collateral evaluation.

5 Conclusions

We have developed an automatic technique to compute a collateral circulation score with an overall 82.2% accuracy. To the best of our knowledge, this is the first time that a computer-assisted classification method has been used for this application, and it is the first step towards helping radiologists and neurosurgeons more efficiently and accurately determine the best course of treatment and predict patient outcomes.

References

1. Sharma, V.K., Teoh, H.L., Wong, L.Y., Su, J., Ong, B.K., Chan, B.P.: Recanalization therapies in acute ischemic stroke: pharmacological agents, devices, and combinations. Stroke Res. Treat. **2010** (2010)
2. Sung, S.M., Lee, T.H., Cho, H.J., Kang, T.H., Jung, D.S., Park, K.P., Park, M.K., Lee, J.I., Ko, J.K.: Functional outcome after recanalization for acute pure M1 occlusion of the middle cerebral artery as assessed by collateral CTA flow. Clin. Neurol. Neurosur. **131**, 72–76 (2015)
3. Ramaiah, S.S., Mitchell, P., Dowling, R., Yan, B.: Assessment of arterial collateralization and its relevance to intra-arterial therapy for acute ischemic stroke. J. Stroke Cerebrovasc. **23**, 399–407 (2014)
4. Cuccione, E., Padovano, G., Versace, A., Ferrarese, C., Beretta, S.: Cerebral collateral circulation in experimental ischemic stroke. Exp. Transl. Stroke Med. **8**, 2 (2016)
5. Pexman, J.H.W., Barber, P.A., Hill, M.D., Sevick, R.J., Demchuk, A.M., Hudon, M.E., Hu, W.Y., Buchan, A.M.: Use of the alberta stroke program early CT score (ASPECTS) for assessing CT scans in patients with acute stroke. Am. J. Neuroradiol. **22**, 1534–1542 (2001)
6. Fonov, V., Evans, A.C., Botteron, K., Almli, C.R., McKinstry, R.C., Collins, D.L., Brain Development Cooperative Group: Unbiased average age-appropriate atlases for pediatric studies. Neuroimage **54**, 313–327 (2011)
7. Cui, X., Huang, J., Zhang, S., Metaxas, Dimitris N.: Background subtraction using low rank and group sparsity constraints. In: Fitzgibbon, A., Lazebnik, S., Perona, P., Sato, Y., Schmid, C. (eds.) ECCV 2012. LNCS, vol. 7572, pp. 612–625. Springer, Heidelberg (2012). doi: 10.1007/978-3-642-33718-5_44

8. Lin, Z., Chen, M., Ma, Y.: The augmented Lagrange multiplier method for exact recovery of corrupted low-rank matrices. https://arxiv.org/abs/1009.5055
9. Turk, M., Pentland, A.: Eigenfaces for recognition. J. Cogn. Neurosci. **3**, 71–86 (1991)
10. Faruqe, M.O., Hasan, M.A.: Face recognition using PCA and SVM. In: Proceedings of the 3rd International Conference on Anti-Counterfeiting, Security, and Identification in Communication, pp. 97–101 (2009)